



Estimation of urban heat island intensity and trends in Spanish cities

M. Ángeles García¹ · Isidro A. Pérez¹

Received: 30 October 2025 / Accepted: 28 February 2026
© The Author(s) 2026

Abstract

Studying urban heat islands (UHIs) in Southern Europe is crucial, as they amplify heat risks under climate change. UHIs and their temporal variability at seven urban–rural pair locations in Spain were analysed from 1970 to 2023. The UHI was defined as the air temperature difference between each urban site and its neighbouring rural sites, and trends were analysed using the non-parametric Mann–Kendall test with Sen’s slope estimator. Based on daily minimum air temperature data, results indicated a mean UHI intensity ranging from -0.15 °C in Alicante to 2.28 °C in A Coruña. The UHI annual trend was significant, increasing in Valladolid (0.023 °C/year) and Alicante (0.009 °C/year) and decreasing in Santander (-0.015 °C/year). Seasonal analysis showed statistically significant trends in Valladolid, particularly in spring and summer (0.029 °C/year). In Alicante, an increase of around 0.012 °C/year was observed in spring and summer, while Madrid showed a trend of 0.012 °C/year in winter. However, a warming effect at the rural site was identified in Barcelona (-0.028 °C/year in autumn) and in Santander (-0.025 °C/year in spring and summer), corresponding to negative UHI trends. The influence of synoptic patterns on UHI yielded values between 3 and 4 °C in A Coruña and Madrid for anticyclonic southeasterly, anticyclonic southerly, and southeasterly air flows. Lower intensities were found in Barcelona (2.5 °C) and were associated with hybrid anticyclonic westerly flows. UHI intensities below 2 °C were obtained at the other locations, with the lowest values being linked to hybrid cyclonic westerly and cyclonic north-westerly flows.

Keywords Climate change · Mann–Kendall test · Minimum temperature · Trend · Synoptic patterns · Urban heat island

1 Introduction

Cities modify the physical environment where they are situated through changes in the natural landscape, and anthropogenic activities have a significant impact on environmental conditions, since they are sources of heat and air pollution (Cuadrat et al. 2022). Urban areas are an important contributor to climate change, with the so-called “urban heat island” or UHI having come to prominence. UHIs have become a major concern in almost every urban area since they refer to the warmer air temperature in urban areas compared to the surrounding rural areas (Arnds et al. 2017; Jabbar et al. 2023; Maqueda et al. 2020; Ward et al. 2016). This effect is mainly evident in minimum daily temperatures, as reported in other studies (Cuerdo-Vilches et al. 2023; Martín-Vide

and Moreno-García 2020; Moreno-García 1994). Different studies have indicated that the geographical location and characteristics of each area studied—such as population density, industrialisation, vegetation cover, and urban morphology—are key factors in the potential urban heat island effect. This suggests the need for local studies aimed at determining the greater or lesser importance of the urban heat island, depending on the type of city in question (Cuerdo-Vilches et al. 2023; Runnalls and Oke 2000; Santamouris et al. 2001; Tzavali et al. 2015). Moreover, UHI intensity is controlled by meteorological conditions such as cloudiness, wind, precipitation, radiation, and pressure, which play a key role in its regulation (Martinelli et al. 2020; Macintyre et al. 2021; Tehrani et al. 2024; Tzavali et al. 2015). As climate change leads to more frequent and intense heat events, these meteorological factors interact with urban characteristics, influencing the urban climate and resulting in significant risks to human health and thermal comfort. Heatwaves, in particular, increase heat stress among high-risk individuals (Ward et al. 2016).

✉ M. Ángeles García
magperez@uva.es

¹ Department of Applied Physics, University of Valladolid,
Paseo de Belén 7, 47011 Valladolid, Spain

At a local or global scale, the impact of UHIs is diverse and includes both positive and negative effects. This urban phenomenon can impact the well-being and health of city dwellers due to direct heat risk or through warmer temperatures during colder periods (Cuadrat et al. 2022; Cuerdo-Vilches et al. 2023; WHO 2021). Not only thermal discomfort but also environmental deterioration can affect many people and can cause increased health and mortality problems (Santamouris and Kolokotsa 2015). Furthermore, the UHI effect can also lead to higher energy demands in buildings due to the need for cooling (Santamouris 2020). Elevated temperatures can also increase the urban pollutant concentration, particularly ground-level ozone and urban smog, since photochemical reactions are intensified (Tzavali et al. 2015). The synergistic effect between high temperature and air pollution can also damage and shorten the operational lifetime of materials.

UHIs have been widely studied for different cities all over the world, particularly in Europe, North America, and Asia, based on both remote as well as in-situ observations that have established their space–time variability (Marando et al. 2019; Santamouris 2020; Tzavali et al. 2015; Wang et al. 1990; Ward et al. 2016). The main controlling factors to have been studied are the impact of urbanization, vegetation, urban area population, climate, season, time of day, and period of time, and which determine UHI intensity (Martinelli et al. 2020; Yue et al. 2019). In European cities, UHI magnitude varies from 1 to 10 °C, with an average maximum value close to 6 °C (Santamouris 2020). UHI magnitude may vary between 0.5 and 11 °C, with an average value close to 4.1 °C for Australian and Asian locations (Santamouris 2015). Several studies have been conducted in Spanish cities (Cuadrat and Martín Vide 2007; Lehoczky et al. 2017) such as Madrid and have shown an average urban heat island intensity of around 2 °C (Almendros and López 1995; Yagüe et al. 1991), with maximum values reaching up to 5 °C (Sobrino et al. 2009). In Granada, higher values have been observed in winter –ranging from 3 to 7 °C– while lower differences of around 0.5 °C have been recorded in autumn and summer (Montávez et al. 2000). On the Mediterranean coast, cities such as Barcelona, Valencia, Castellón, and Alicante have reported maximum intensities of up to 7 °C and average values of around 4 °C (Moreno and Serra 2016).

As another important controlling factor, certain synoptic weather patterns can cause the behaviour and range of changes in UHI intensity as local meteorological parameters are modified (Yang et al. 2022). It is therefore important to obtain the features of the UHI under different synoptic situations and to determine those which intensify the UHI (Aquino-Martínez et al. 2025; Hardin et al. 2018). Studying the interaction between UHI and synoptic patterns is crucial

for understanding changes in urban climate (Aquino-Martínez et al. 2025; Colangelo et al. 2022). There are different procedures to determine synoptic conditions based on traditional or machine learning techniques (Su et al. 2018). This study explores the role and impact of synoptic patterns using surface pressure. The procedure applies the Lamb weather classification, which has been satisfactorily used mainly for anticyclonic situations linked to the strongest UHI intensities (Pérez et al. 2024).

Additionally, green spaces can constitute a differentiating factor when studying urban phenomena. The World Health Organization (WHO) recommends increasing green space for health and environmental benefits. Local studies can thus help to determine the importance of city features in establishing the key factors that influence the potential urban heat island effect, added to which the combination of different factors should also be considered.

Although the UHI has been extensively studied, understanding of the processes involved remains incomplete. It is important to characterise the UHI at different locations. This paper establishes specific aims to provide deeper insights into the climate variability that affects the urban environments examined. Temperature trends were analysed at different urban and nearby rural locations across Spain, specifically in coastal and inland areas, as well as medium-sized and large cities, some of which had not previously been studied. UHI intensity and temporal variability were also assessed, including an interdecadal analysis, the relationship with heatwave periods, and trend estimation using a non-parametric test. The influence of atmospheric pressure was examined by analysing synoptic patterns based on the Lamb classification method, which is considered a key factor influencing urban heat islands. Finally, UHI trends were compared among the study areas.

This study aims to improve current knowledge of the urban heat island in the Mediterranean region and could help authorities to develop control strategies and effective policies to better manage temperature variations in urban areas. European cities must adapt to climate change and implement green infrastructures if they are to reduce the effects of UHI, protect biodiversity, and improve air quality for public health, particularly in view of urban growth and ever-increasing urban heat stress.

2 Material and methods

2.1 Sampling site and data

The Iberian Peninsula within the Mediterranean basin is diverse and presents different climatic conditions. The southern half of the Peninsula is characterised by a Mediterranean

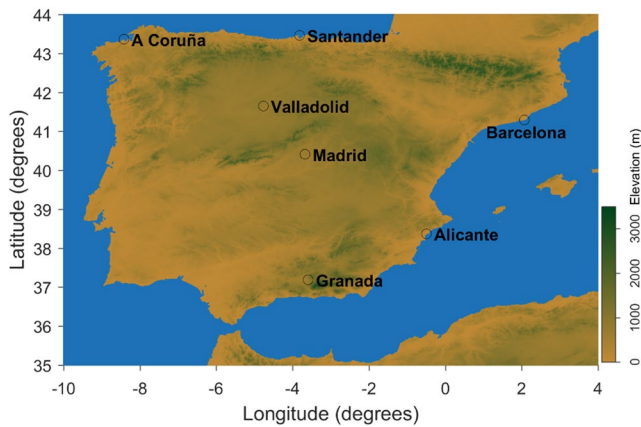


Fig. 1 Map of the Iberian Peninsula indicating the sites analysed and the elevations

Table 1 Main features of the meteorological stations

Station	Latitude (deg:min:sec)	Longitude (deg:min:sec)	Elevation (m)	Period	Distance (km)
A Coruña	43:22:01	-008:25:09	58	1970–2023	6.4
A Coruña-Airport (Alvedro)	43:18:24	-008:22:18	98	1972–2023	
Alicante	38:22:11	-000:29:39	81	1970–2023	8.8
Alicante-Airport (El Altet)	38:16:58	-000:34:14	43	1970–2023	
Granada-Cartuja	37:11:22	-003:35:44	775	2010–2023	15.0
Granada-Airport (García Lorca)	37:11:22	-003:47:21	567	1973–2023	
Santander	43:27:52	-003:49:08	64	1970–2023	5.0
Santander-Airport (Parayas)	43:25:45	-003:49:53	5	1970–2023	
Valladolid	41:39:00	-004:46:00	735	1974–2023	10.8
Valladolid-Airport (Villanubla)	41:42:00	-004:51:00	846	1970–2023	
Madrid-Retiro	40:24:42	-003:40:41	667	1970–2023	14.5
Madrid-Airport (Barajas)	40:28:00	-003:33:20	609	1970–2023	
Barcelona-El Raval	41:17:34	+002:04:11	4	1999–2023	12.0
Barcelona-Airport (El Prat)	41:23:02	+002:10:00	33	1970–2023	

climate, while the northern half is influenced by a Mediterranean oceanic climate. The southeast of the Peninsula has a semi-arid climate, whereas an oceanic climate is found in

mountainous regions (Busenkova et al. 2024). This study is based on sites that are representative of those conditions.

Seven locations in Spain were selected to investigate the effect of the urban heat island (A Coruña, Alicante, Granada, Santander, Valladolid, Madrid, and Barcelona) (see Fig. 1). Two stations for each location were considered: one corresponded to an urban environment, with the other having rural features and being located some distance from the corresponding city. Four sites are on the coast: A Coruña and Alvedro; Alicante and Altet; Barcelona-El Raval (henceforth referred to as Barcelona) and Barcelona-Airport; Santander and Parayas. The other three are inland: Madrid-Retiro (henceforth referred to as Madrid) and Madrid-Airport; Granada and Granada-Airport; Valladolid and Villanubla. The selected locations involved the largest cities such as Madrid (3,277,000 inhabitants) and Barcelona (1,628,000 inhabitants), mid-sized cities (less than 500,000 population) such as A Coruña, Alicante, Granada, and Valladolid, and Santander with a population of under 200,000 inhabitants.

Each study location therefore has a different associated climate according to the Köppen-Geiger climate classification. The most dominant climate is Csa (hot-summer Mediterranean climate), which extends to Valladolid, Granada, and Barcelona, and which is characterised by warm or hot summers and cold, wet winters. A Coruña has Csb (warm-summer Mediterranean climate), and Santander is dominated by the Cfb (Oceanic climate), both of which are predominant in the north of Spain. Madrid exhibits a Mediterranean to cold semi-arid climate (Csa and BSk, respectively), while Alicante is linked to the BSk climate type (semi-arid) (Agencia Estatal de Meteorología-España and Instituto de Meteorología-Portugal 2011; Bushenkova et al. 2024, Salvati et al. 2017).

The geographical features of the stations are presented in Table 1, which also includes the distance between each urban site and its corresponding rural site –ranging from approximately 5–15 km. The height of the stations above mean sea level varies significantly across areas, and ranges from 4 to 846 m. Each pair of sites is geographically comparable for studying the UHI (Martínez 2014).

With some exceptions –as can be seen in Table 1– the study is based on the period 1970–2023, using daily data of the different meteorological variables; namely, mean temperature, maximum temperature, and minimum temperature. Data were obtained from ECA&D (European Climate Assessment & Dataset), which is available at the link <https://www.ecad.eu/dailydata/predefinedseries.php>. Data availability is greater than 98%, except for Granada-Airport, which is 92%.

Local meteorological conditions present a wide variety of features which are attributed, among other reasons, to

population density, land use, and topography. A Coruña is in northwest Spain on a gulf on the Atlantic Ocean and has a flat isthmus and soft hills around the city. Situated in northern Spain, the city of Santander is defined by the Cantabrian coastline and the Bay of Santander, with a pre-coastal plain where some mountains rise up. Valladolid is on the northern Spanish plateau, in the centre of the Duero sedimentary basin along the Pisuerga River, and is surrounded by mountains, except to the west, where the absence of large mountains allows an open corridor to the Atlantic Ocean. Granada is in southern Spain, at the foot of the Sierra Nevada mountains and at the confluence of some rivers in a valley. Madrid lies in the centre of the Iberian Peninsula, on the southern plateau. It is close to the Guadarrama mountain range and extends over the Manzanares and Jarama basins. Barcelona is located on the northeastern Mediterranean coast of the Iberian Peninsula, on a plain bordered by the Besós and Llobregat rivers, near the Serra de Collserola mountain range. Alicante is on the southeastern coast of Spain and is surrounded by mountainous landscapes with the Serra de Fontcalent to the west.

2.2 Mann–Kendall test and Sen’s slope method

The procedure used in this research to quantify urban heat island intensity is based on the daily temperature difference between urban and rural (Eq. 1), with the air temperature in the city usually being higher than the temperature of the nearby non-urban area (Cuadrat et al. 2022; Oke 1973); in other words:

$$UHI = \Delta T_{u-r} = T_u - T_r \quad (1)$$

where ΔT_{u-r} is the intensity of the heat island, UHI, T_u is the temperature of the urban station, and T_r is the temperature of the rural station.

Using the daily values of the corresponding temperature parameters, a temporal analysis of the UHI was carried out to observe its behaviour at different locations. The statistical approach involved applying the Mann–Kendall test and Sen’s slope to identify and assess the magnitude of the trends over time in annual values of the variables studied. These methods were run using MAKESENS 1.0, developed by the Finnish Meteorological Institute (Salmi et al. 2002). Estimation of the slope applied a linear model using a non-parametric procedure (Kundan et al. 2020; Sen 1968). Following the procedure described, the Mann–Kendall test statistic, S , is calculated using Eq. 2.

$$S = \sum_{i=1}^n \sum_{j=i+1}^n \text{sign}(x_j - x_i) \quad (2)$$

where n is the total number of data values, and x_i and x_j are the annual values. For large samples ($n > 10$), the test uses a normal distribution approximation (Z statistics). The significance levels tested are 0.001, 0.01, 0.05 and 0.1.

The study was completed by estimating the slope of the trend. The method used was developed by Sen (1968) and is assumed to be linear as a function of time:

$$f(t) = Qt + B \quad (3)$$

where B is a constant and Q is the slope.

2.3 Synoptic situation analysis

A synoptic climatological classification using surface pressure was carried out to determine the prevailing meteorological conditions linked to the urban heat island values. The method determines the synoptic weather types following the procedure given by Lamb (1972). The expression applied is shown in Pérez and García (2023), in accordance with the method provided by Jones et al. (2013) for sea level pressure series, available at the NOAA PSL, Boulder, Colorado, USA website (<https://psl.noaa.gov>). The study area covers the Iberian Peninsula, and synoptic weather types comprise cyclonic or anticyclonic, pure directional types, hybrids, and unclassified type (Table S1) (García et al. 2024).

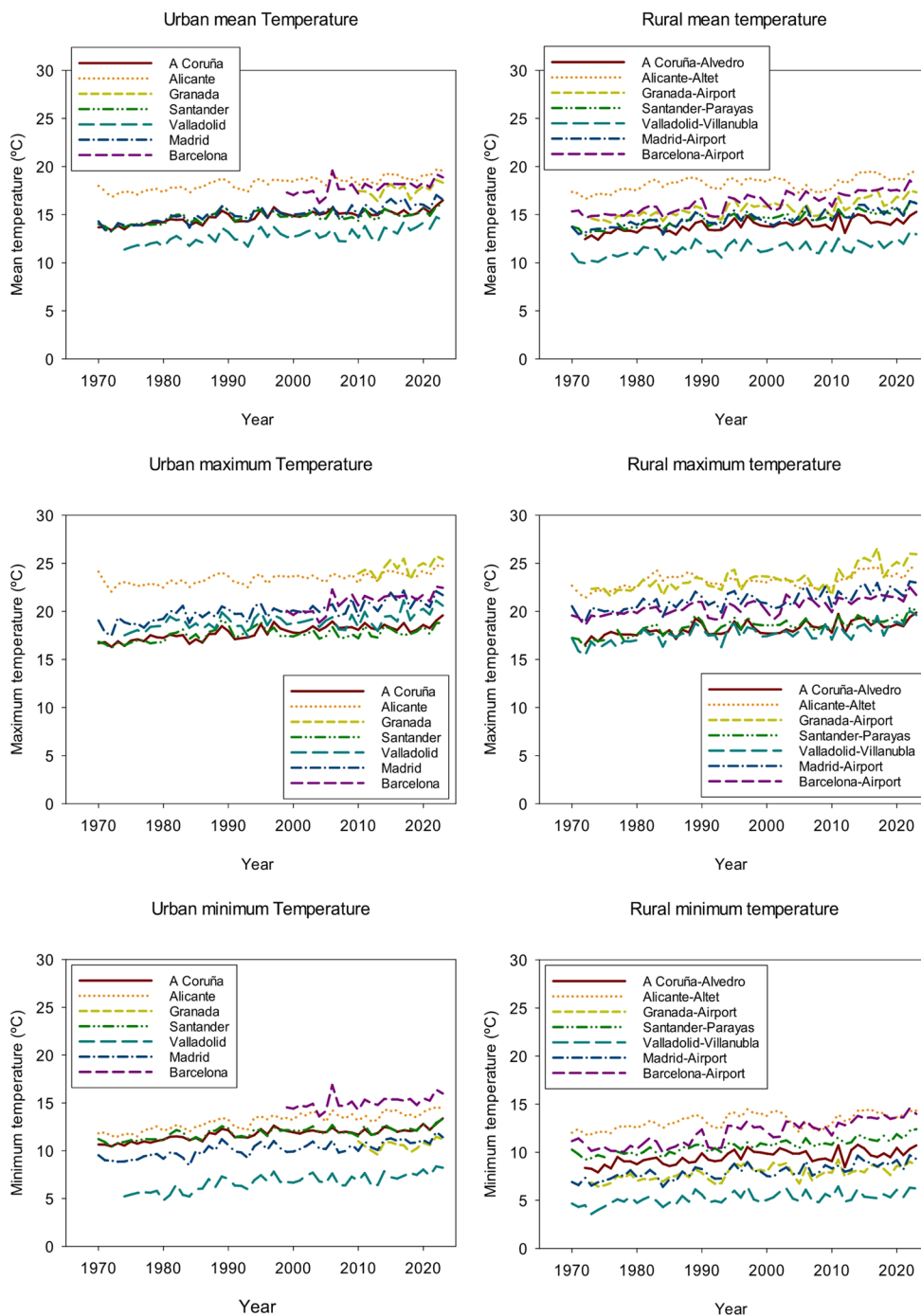
3 Results and discussion

3.1 Annual temperature trend analysis

The annual mean, maximum, and minimum temperatures for the whole period of study were analysed and plotted in Fig. 2 for the urban and rural stations. Mean urban temperature values ranged from 11.4 °C in Valladolid to 19.6 °C on the Mediterranean coast (Alicante and Barcelona). Lower values were obtained for the rural sites, especially for the extreme low values, with a difference of about 1.5 °C being observed in Valladolid and Barcelona. Maximum temperatures were between 16.2 °C in Santander and 25.7 °C in Granada, and 15.4 and 26.6 °C at Valladolid-Airport and Granada-Airport, respectively. Minimum temperatures showed high values at urban sites, with extreme values between 4.8 and 16.9 °C, corresponding to inland areas (Valladolid) and Mediterranean coast sites (Barcelona), respectively, compared to 3.6 to 14.6 °C obtained in rural environments.

The test results for estimating temperature trends over the whole study period (in general over 54 years, except 14 for Granada and 25 for Barcelona) are shown in Table 2. All temperature parameters increased, since Z values were

Fig. 2 Annual temperatures over the period 1970–2023 for the urban (left) and rural (right) stations



positive and statistically significant at the 0.001 significance level, except those obtained for Granada, which had lower values or even no significance for the minimum temperature.

As regards mean temperature, the highest increase trends were observed at the Granada site, with values up to 0.067 °C/year for the urban site and slightly lower for the rural site (0.048 °C/year), at the Barcelona stations, reaching 0.059 °C/year, and at the Madrid stations, which were no lower than 0.043 °C/year. However, the urban Santander station presented the lowest trend, 0.026 °C/year. Trend estimations

in the remaining stations ranged from 0.03 to 0.039 °C/year. A similar pattern was observed for the maximum temperature, with the highest intensity trend being reached at the Barcelona station (0.1 °C/year), followed by the Granada urban and rural sites (0.092 and 0.055 °C/year, respectively) and the Madrid urban and rural stations (0.051 and 0.047 °C/year, respectively). The lowest values were found in Santander (0.022 °C/year) and Alicante (0.025 °C/year). Trends at the remaining locations ranged between 0.029 and 0.043 °C/year. Minimum temperature trends ranged

Table 2 Temperature trend analysis at the different sites (Q (°C/year) and B (°C)) for the mean, maximum, and minimum temperatures

Station/Test	T_{mean} T_{Mean}			T_{Maximum}			T_{minimum}		
	Test Z	Q	B	Test Z	Q	B	Test Z	Q	B
A Coruña	6.97	0.037	13.75	6.73	0.039	16.77	6.76	0.034	10.77
A-Coruña-Airport	5.85	0.030	13.01	5.67	0.030	17.37	5.04	0.032	8.76
Alicante	6.68	0.038	17.30	5.16	0.025	22.97	7.28	0.049	12.09
Alicante-Airport	4.83	0.032	17.38	4.07	0.029	22.29	5.12	0.036	12.41
Granada	1.86	0.067	17.29	2.41	0.092	24.01	0.88	0.038	10.44
Granada-Airport	5.85	0.048	14.55	5.41	0.055	22.07	4.59	0.033	6.97
Santander	4.91	0.026	13.98	4.05	0.022	16.81	5.45	0.028	10.99
Santander-Airport	6.80	0.042	13.34	5.86	0.043	17.23	7.48	0.041	9.53
Valladolid	4.86	0.039	11.80	3.39	0.029	18.19	5.36	0.047	5.49
Valladolid-Airport	5.36	0.033	10.51	5.28	0.041	16.60	4.76	0.022	4.48
Madrid	6.71	0.046	13.86	6.34	0.051	18.64	6.60	0.041	9.08
Madrid-Airport	6.40	0.043	13.41	5.79	0.047	19.92	6.16	0.038	6.98
Barcelona	3.74	0.059	17.12	3.62	0.10	19.81	3.53	0.053	14.41
Barcelona-Airport	7.16	0.058	14.66	6.25	0.042	19.45	5.04	0.060	7.80

Significance levels are 0.001, except for Granada, where they are 0.1 (mean temperature), 0.05 (maximum temperature), and >0.1 (minimum temperature)

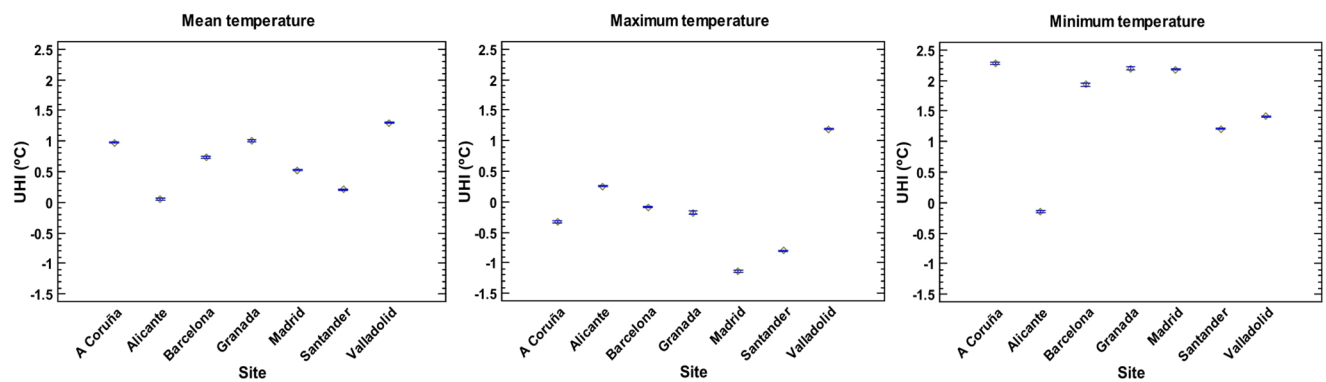


Fig. 3 Means and 95% Fisher LSD (Least Significant Difference) of daily UHI for each site at the study period associated to mean, maximum, and minimum temperatures

from 0.022 °C/year in Valladolid to 0.060 °C/year at Barcelona-Airport, with the greatest differences being observed between the Valladolid stations. The trends of the rural stations in Santander and Barcelona were higher than those for the corresponding urban ones. These results may reflect the sea's moderating influence on urban sites, combined with land-use changes and greater sensitivity of rural areas to regional warming.

The cities analysed showed increasing temperature trends –around 0.04 °C/year– with higher values at the urban sites, except for certain exceptions where rural values stood out, such as Santander, for the three temperature indicators, Alicante and Valladolid for the maximum temperature, and Barcelona for the minimum temperature. These results concur with Roca et al. (2023), who reported increases in the main Spanish cities of around 2.17 °C.

3.2 Urban heat island (UHI)

The urban heat islands for the sites selected are presented in Fig. 3 using mean plots. As can be observed, the UHI presents very low average values for the mean and maximum temperatures, being no higher than 1 °C. However, the difference is particularly noticeable for minimum temperatures, since urban points cool to a lesser degree than the nearby rural areas (Maqueda et al. 2020). The average UHI in most of the sites was between 1.2 and 2.2 °C, except in Alicante where there was virtually no difference in minimum temperatures. Considering the results showing the larger effect of the minimum temperature on UHI intensity, from this point forward the UHI corresponding to the minimum temperature for each site will be considered.

There were statistically significant differences in average UHI values between the locations studied, except for the 2.2 °C obtained in Madrid and Granada. The topographical setting of Granada in a relatively enclosed valley can limit

air circulation, resulting in elevated nighttime temperatures and mean UHI intensity. However, Madrid exhibited higher extreme values (between -6.1 and 11.7 °C). These intensities are within the range of other studies (Maqueda et al. 2020; Núñez et al. 2017; Román et al. 2017; Yagüe et al. 1991). Fernández et al. (1996) investigated the effect of topography for Madrid, mainly in the valleys (Manzanares River) where cold air accumulates on winter nights with strong radiation, and which are the preferred routes of air penetration from the surrounding areas. The UHI can be explained by the topography of the city and the high density of buildings, which together causes heat retention. The average UHI intensity in A Coruña, which is an open coastal area, was slightly higher at 2.3 °C (ranging from -9.6 to 10.0 °C). The city retains heat overnight, while the surrounding areas remain relatively cool. The UHI estimated in Barcelona was approximately 1.9 °C on average, with extreme values of -7.4 and 12.3 °C for the whole study period. These results are consistent with those obtained by Martín-Vide and Moreno-García (2020), who evaluated urban heat island intensity in Barcelona and established a value of about 2.0 °C for a ten-year period. Moreno-García (1994) also reported a maximum intensity of the urban heat island effect of about 8 °C, based on minimum temperatures. Urban temperature and ventilation in Barcelona are influenced by the city's proximity to the Serra de Collserola mountain chain and to the Mediterranean Sea (Salvati et al. 2017). A lower mean UHI value was obtained in Valladolid, 1.4 °C (ranging from -8.6 to 8.6 °C), considering its location on the Northern Spanish Plateau and its setting in a valley. Santander is a coastal city with maritime influence, which favours ventilation and which may limit UHI intensity, where the lowest mean value of 1.2 °C (ranging from -6.2 to 12.6 °C) was observed. A barely noticeable average heat island yielding a negative mean was obtained in Alicante, -0.15 °C (with some extreme intensities between -9.0 and 6.2 °C), in part due to the negative average values in most years, except from 2003 to 2010 and the last four years. A similar result was attributed by Martínez (2014) to the characteristics of the area where the airport is located

–the rural site– since it is warmer because of the Serra de Fontcalent and the Foehn effect that causes the warm thermal anomaly in the zone. This effect was also detected in Jato-Espino (2019), suggesting higher values at rural stations in the Mediterranean area, particularly in Alicante.

Overall, these findings highlight that UHI intensity is not only a function of urban density but is also influenced by geographical setting, local airflow patterns, and topographical features. The results found in the areas studied are also comparable to those reported for other locations in Europe, such as Hamburg with 1.2 °C (Arnds et al. 2017), and the values reported for larger cities like London, around 1.8 °C (Pérez et al. 2024; Wilby 2003).

3.2.1 Annual trend analysis

This research aims to analyse annual trends in UHI intensity by applying the Mann–Kendall statistical test to differences in minimum temperatures between urban and rural locations. Sen's slope statistics were then used to estimate the magnitude of the trend. The test results shown in Table 3 reveal that annual UHI trends were only statistically significant in Alicante, Santander, and Valladolid for a significance level of 0.001. The annual trend value was quite high in Valladolid (0.023 °C/year). Lower values were found for the other two stations, with a different effect. While UHI increased in Alicante at a rate of 0.009 °C/year, it decreased in Santander with a similar rate of -0.015 °C/year. The rest of the stations showed no statistically significant annual trend. However, a warming effect was found in Granada, A Coruña, and Madrid. The result for Madrid concurs with other studies for a similar period where a non-significant positive trend in Madrid and at the Airport (Barajas) was determined, albeit with a lower value (Maqueda et al. 2020). In contrast, Barcelona experienced a warming effect in its surrounding areas. Studies carried out by Martín-Vide and Moreno-García (2020) also show a slight decreasing trend in UHI intensity in Barcelona. Urban structure and population variations over the years –particularly the slight decrease in recent years– have had a major impact on how the UHI has developed, although this has also been shaped by the geographical features of the locations and by weather conditions (Jabbar et al. 2023).

The interdecadal study (five decades) showed that the highest mean UHI values were observed in recent years, beginning in 2020, coinciding with the increased intensity of heatwaves across the different locations. Madrid also showed high values during the 1980–1989 decade. Furthermore, mean UHI values in Valladolid have increased since 1980.

Table 3 Mean values of UHI and the annual trend analysis associated to differences in minimum temperatures at the different sites

Station/Test	UHI- T_{minimum}				
	Mean (°C)	Test Z	Significance	Q (°C/year)	B (°C)
A Coruña	2.28	0.4		0.002	2.23
Alicante	-0.15	3.57	0.001	0.009	-0.57
Granada	2.20	0.66		0.023	1.26
Santander	1.21	-4.86	0.001	-0.015	1.64
Valladolid	1.41	6.61	0.001	0.023	0.80
Madrid	2.18	0.29		0.001	2.14
Barcelona	1.93	-1.52		-0.021	2.13

Blank significance level: >0.1

3.2.2 Seasonal trend analysis

A temporal analysis was also conducted by seasons and confirmed some singularities of the sites (see Table 4). The mean UHI intensity for A Coruña in winter and autumn was around 2.6 °C and 1.9 °C in spring and summer. Although the mean UHI value for Granada in autumn was 2.5 °C, the results in summer and winter were also noteworthy (2.4 and 2.3 °C, respectively). To a lesser extent, the mean value found in spring was 1.6 °C. The highest intensities in Barcelona were recorded in autumn and winter (approximately 2.4 °C), while the lowest were in summer and spring, and were around 1.5 °C. There were few differences in UHI seasonal intensities in Madrid, although winter was associated with the highest mean UHI value of 2.4 °C. However, the lowest UHI values were observed in spring, and were around 2 °C. In Santander, there was a difference of about 0.8 °C in UHI values, reaching 1.6 °C in winter and autumn. In contrast, the UHI in Valladolid was slightly higher in spring and summer –around 1.6 °C– yielding a difference of about 0.5 °C compared to the values obtained in winter and autumn. Alicante behaved differently, as UHI intensities exhibited negative values in summer and autumn, and positive values in winter and spring, ranging from −0.40 °C in summer to 0.12 °C in spring, although these values were not very high.

In general, autumn and winter showed greater UHI intensities at all the sites, except for Valladolid. UHI intensities in A Coruña and Santander were similar to those observed in other nearby Atlantic coastline cities in Portugal –Lisbon and Porto (Andrade et al. 2023). The authors found stronger UHI in winter, associated not only with anthropogenic changes but also with meteorological conditions such as sea breeze that affected local events. In Granada, high values were found in autumn and winter and even in summer. Results confirmed that they were influenced by regional or local climate, urban characteristics, and the location of the meteorological station, which is situated in the warmest part of the city (Martinelli et al. 2020; Montávez et al. 2000). Hidalgo and Arco (2022) also attributed the stronger UHI during winter and autumn in Andalusian cities to local climate conditions, including radiation and wind characteristics, as well as the city structure. There was little contrast in UHI seasonal intensities in Madrid, although winter is associated with the highest mean UHI value, as also reported by Maqueda et al. (2020). Faster cooling of rural areas, combined with anticyclonic conditions and the thermal inertia of buildings, which release heat more slowly at night, may contribute to this result. However, the lowest UHI value was obtained in spring and was associated to greater air mixing (convection and winds), which reduces the temperature difference between the city and the surrounding areas. The highest UHI intensities found in Barcelona in autumn

Table 4 Mean UHI values and seasonal trend analysis during the study period

Station/Season	Winter			Spring			Summer			Autumn		
	Mean (°C)	Test Z	Trend (°C/year)	Mean (°C)	Test Z	Trend (°C/year)	Mean (°C)	Test Z	Trend (°C/year)	Mean (°C)	Test Z	Trend (°C/year)
A Coruña	2.65	0.94	0.005	1.93	1.73	0.006	1.94	-1.02	-0.004	2.58	-0.72	-0.004
Alicante	0.03	0.90	0.004	0.12	3.04	0.011	-0.40	5.83	0.019	-0.35	2.77	0.012
Granada	2.27	1.20	0.084	1.59	0.11	0.009	2.39	0.11	0.004	2.53	0.99	0.048
Santander	1.58	0	0	0.77	-5.71	-0.024	0.91	-6.97	-0.025	1.58	-2.50	-0.009
Valladolid	1.19	4.77	0.020	1.68	5.89	0.029	1.64	7.02	0.029	1.13	4.77	0.020
Madrid	2.37	1.73	0.012	1.96	-0.51	-0.002	2.21	-0.79	-0.005	2.18	0	0
Barcelona	2.45	-0.86	-0.018	1.53	-0.91	-0.016	1.40	-1.89	-0.025	2.36	-1.75	-0.028

significance level 0.001; significance level 0.01; significance level 0.05; significance level 0.1; significance level > 0.1

and winter were also reported in previous studies (Martín-Vide et al. 2020; Salvati et al. 2017) for a short period (nine years). These studies showed that the UHI was weaker in summer because of the sea breeze and, consequently, the stronger intensity was obtained in winter and autumn. Other findings concerning the UHI in Mediterranean coastal cities have confirmed the influence of sea breeze on changes in UHI patterns (Martinelli et al. 2020).

Trend analysis results using the values of Mann–Kendall trend statistics (Z) and trend values (Q) for seasonal series of the annual mean UHI of all stations are also presented in Table 4. The mean winter UHI at Valladolid and Madrid exhibited statistically significant increasing trends with different levels of significance. The trend in Valladolid was significant at the 0.001 significance level, while the trend for Madrid was less significant at the 0.1 significance level. Valladolid showed the highest trend values of $0.020\text{ }^{\circ}\text{C}/\text{year}$ as indicated by the Q statistics compared to $0.012\text{ }^{\circ}\text{C}/\text{year}$ for Madrid. Although Z values were also positive for the rest of the stations except in Barcelona, the trends were statistically non-significant. A statistically significant positive trend in mean spring UHI emerged for A Coruña, Alicante, and Valladolid. The trend for Valladolid was significant at the 0.001 significance level, while trends for Alicante and A Coruña were less significant (at the 0.01 and 0.1 significance levels, respectively). The trend value for Valladolid was $0.029\text{ }^{\circ}\text{C}/\text{year}$, which was greater than that obtained in Alicante ($0.011\text{ }^{\circ}\text{C}/\text{year}$) and A Coruña ($0.006\text{ }^{\circ}\text{C}/\text{year}$). However, Santander showed a statistically significant negative trend at the 0.001 significance level and a rate of $-0.024\text{ }^{\circ}\text{C}/\text{year}$. Similar results were found for the UHI summer mean with certain features. In this season, the trends for Valladolid and Alicante were positive and statistically significant (at the 0.001 significance level) with values of 0.029 and $0.019\text{ }^{\circ}\text{C}/\text{year}$, respectively. Statistically significant negative trends were found for Santander and Barcelona (at the 0.001 and 0.1 significance levels, respectively) with both showing the same estimated rate of $0.025\text{ }^{\circ}\text{C}/\text{year}$. The same behaviour seen in summer was found in Santander and Barcelona for autumn; in other words, a significant and negative trend, albeit with a different statistical significance (at the 0.05 and 0.1 significance levels, respectively) and with a great difference in the values ($-0.009\text{ }^{\circ}\text{C}/\text{year}$ for Santander and $-0.028\text{ }^{\circ}\text{C}/\text{year}$ for Barcelona). These results can be attributed to a combination of climatic and urban factors. In contrast to the behaviour of inland cities, both coastal cities are influenced by the sea, which moderates urban warming. In addition, urban adaptation measures may have reduced heat storage, whereas surrounding rural areas may be warming at a similar or at an even faster rate due to land-use changes.

In general, seasonal UHI intensities increased during the study period, albeit to varying degrees depending on the

city and not always with statistical significance. The heat effect was particularly noticeable in Valladolid in all seasons, while a warming effect in the surrounding areas was observed in Santander (in spring and summer) and in Barcelona (in summer and autumn).

3.3 UHI under different synoptic situations

UHI is influenced by certain synoptic situations that characterise the state of the atmosphere at a given location (Aquino-Martínez et al. 2025). Figure 4 depicts in box-and-whisker plots the distribution of UHI values for the different synoptic patterns identified for each location based on the Lamb classification. In general, the highest mean UHI values were observed under a high-pressure system (anticyclone), which brings fair weather conditions with clear skies, stable conditions, and light winds. Hybrid patterns were also involved, such as anticyclonic southerly (AS), anticyclonic southeasterly (ASE), and anticyclonic southwesterly (ASW), depending on the location. The maximum mean UHI value was obtained in Madrid ($4.2\text{ }^{\circ}\text{C}$), with the greatest range being $4.4\text{ }^{\circ}\text{C}$. A Coruña and Santander showed lower values, with a range of $2.7\text{ }^{\circ}\text{C}$, while Valladolid had a value of $2.3\text{ }^{\circ}\text{C}$. Data variability for most synoptic patterns in Alicante was similar, with the lowest mean UHI values ranging from -1.1 to $0.5\text{ }^{\circ}\text{C}$. Although the range was the same in Granada, all mean values were positive and reached up to $1.5\text{ }^{\circ}\text{C}$. Apart from the size of the city and the location as well as the topographical characteristics of the study sites, the state of the atmosphere proved crucial in the formation of the urban heat island since the results showed some differences related to synoptic conditions.

The most frequent and representative synoptic weather situations are presented in Table 5 together with the associated UHI intensity. The most frequent synoptic patterns were the anticyclonic situation (A), representing more than 21%, and the unclassified situation (U), which comprises no defined air flows and represents about 17.5%. Easterly flow (E) accounted for approximately 7.6%, while the cyclonic pattern (C) was less frequent, at 6.7%. The corresponding UHI intensity for each site linked to the A and U patterns was positive, except for Alicante, which showed a low contrast (-0.21 and $-0.30\text{ }^{\circ}\text{C}$, respectively). In general, higher values were associated with anticyclonic situations (A). As regards the mentioned patterns (A and U types), UHI intensity was greatest in Madrid, reaching 3.19 and $2.69\text{ }^{\circ}\text{C}$, respectively. This was followed by A Coruña, which had very similar values –around $2.3\text{ }^{\circ}\text{C}$ – and Barcelona, where the difference between the two types was about $0.4\text{ }^{\circ}\text{C}$, close to $2.0\text{ }^{\circ}\text{C}$. UHI intensity in Santander for A and U synoptic situations reached 1.72 and $1.18\text{ }^{\circ}\text{C}$, respectively. However, Granada and Valladolid showed no differences between

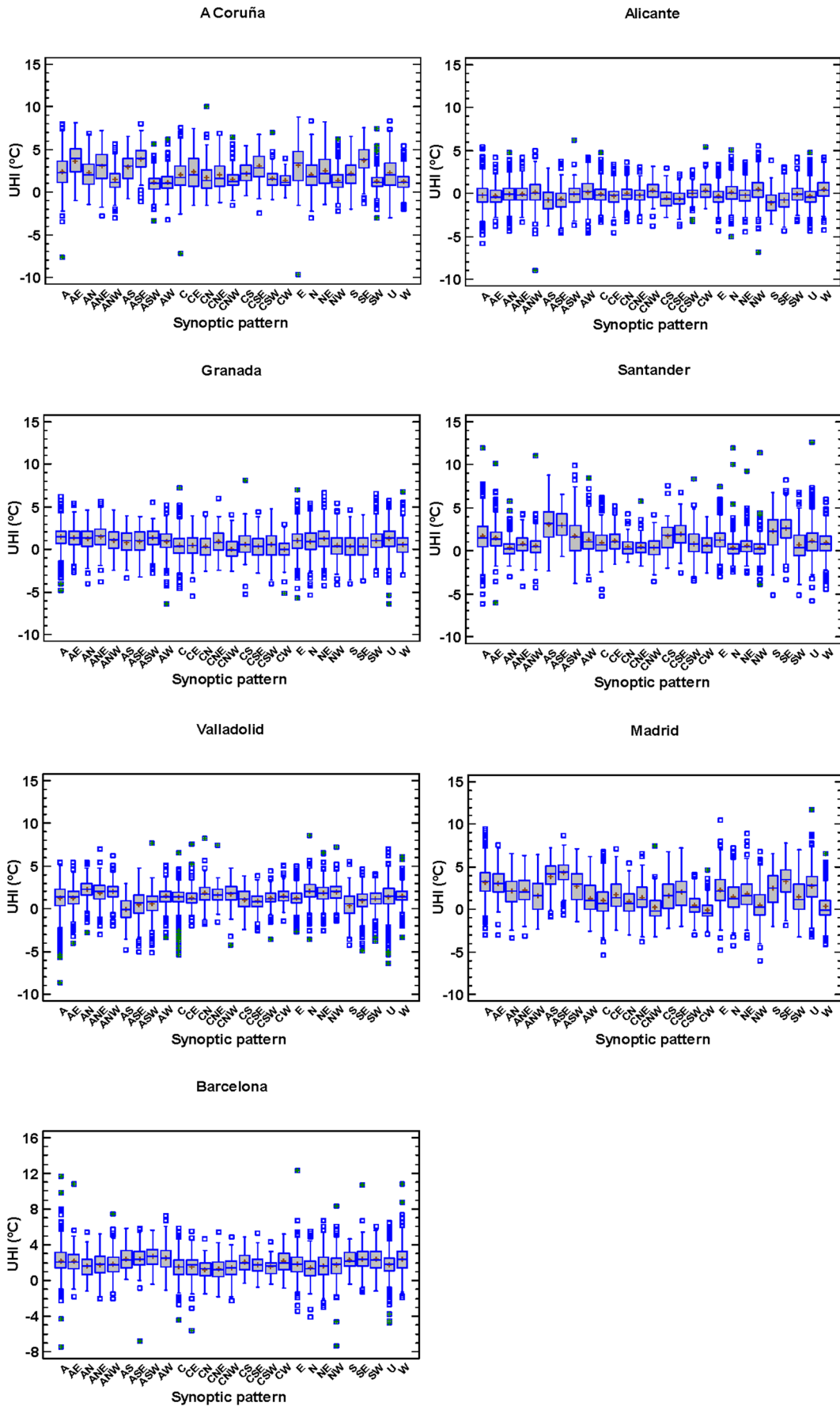


Fig. 4 UHI for different synoptic patterns at each location during the study period. The mean is depicted with a cross sign, the median as a horizontal line, while the upper and lower whiskers extend out to the extreme maximum and minimum values below or above 1.5 times the interquartile range from the first and third quartiles. Outliers are represented as small squares

the two weather types, with values around 1.4 and 1.3 °C, respectively. Eastern flows were associated with high UHI intensity in A Coruña (3.19 °C) and lower values in Madrid and Barcelona (2.29 and 1.86 °C, respectively). This synoptic pattern led to lower UHI intensities at the remaining locations, and which were all below 1.3 °C. The pure cyclonic pattern exhibited low values, except in A Coruña (2.01 °C), Barcelona (1.48 °C), and Valladolid (1.32 °C).

When analysing the results of the highest values of UHI intensity associated with synoptic situations, notable differences were observed. In Madrid, values ranged between 3 and 4 °C associated to anticyclonic situations and ASE or SE hybrid types (see also Table 5). Under these stable conditions, southerly winds linked to warm and dry advections, together with the absence of any significant orographic barriers, intensify the lack of ventilation. This effect, combined with dense urban construction, contributes to a stronger urban heat island (UHI). Almendros and López (1995) also reported that high pressure was linked to relatively intense UHI values in Madrid, whereas low-pressure systems were linked to lower intensities. High values were also observed along the coast—particularly in A Coruña—with an average intensity of 3.6 °C, mainly associated with light winds from inland areas, which are warmer and drier. However, although Santander is also located on the northern coast and is affected by southerly winds—which are more stable and warmer than northerly breezes—it exhibits lower UHI values due to stronger orographic and local wind influences. Unlike A Coruña, Santander is less exposed, with a mean UHI intensity of around 2.7 °C, although the Foehn effect linked to the Cantabrian Range contributes to frequent temperature increases across the area.

In Barcelona, stable anticyclonic conditions limit the dispersion of heat accumulated in buildings and pavements. Weak offshore winds (W-SW) enhance the thermal contrast between the city and its surroundings and may inhibit the intrusion of cooler marine air, thereby maintaining high temperatures. Weak SE winds may also sustain nocturnal urban heat. The ASW and AW situations produce the highest UHI intensities, reaching around 2.7 °C (with an average of approximately 2.5 °C for the highest values). These findings are consistent with the results reported by Martín-Vide et al. (2016) for the Barcelona area over a short study period.

An average UHI intensity of around 2 °C was observed in Valladolid, reflecting not only the influence of anticyclonic conditions but also NW or even N flows which, due

to the configuration of the Pisuegra Valley where the city is located, are channelled and decelerate within the urban canopy, thereby reducing ventilation. In addition, atmospheric stability favours nocturnal thermal inversions, causing the heat accumulated in the city to be released more slowly. Southerly flows do not intensify the urban heat island because, although they are warmer, they are also more unstable and reduce the thermal contrast between the city and its surroundings.

In Granada, the factors favouring the highest urban heat island values are related to anticyclonic conditions and to the circulation of air around the city, which is influenced by its location within a valley. N and NE winds, associated with high atmospheric stability, promote nocturnal thermal inversions, weaken upon entering the city, and limit effective ventilation. Mean urban heat island values are around 1.4 °C, showing a marked contrast with the other cities.

A weak urban heat island effect is observed in Alicante, with a mean intensity of 0.4 °C, and which is mainly influenced by maritime effects and favourable topography that result in small temperature differences between the urban centre and its surroundings. The predominant synoptic situations are hybrid cyclonic conditions and westerly flows. The influence of synoptic situations in some Mediterranean coastal cities differs from that observed in continental environments or, as previously noted, in Barcelona. In Alicante, UHI intensity is significantly enhanced during cyclonic situations, hybrid, and W and NW flows, as a result of the interaction between synoptic-scale atmospheric circulation, proximity to the sea, and the thermal properties of the urban environment, which cause the city to retain more heat than its surroundings (Martínez 2014).

4 Conclusions

UHI intensity was studied at seven urban–rural paired sites in Spain using temperature datasets for the period 1970–2023. Locations included coastal and inland cities, and differed in population density, climate, and topographical features. Results showed that urban temperatures increased significantly at all sites, with magnitudes greater than those of the corresponding rural temperatures, except in Santander, for maximum temperatures in Alicante and Valladolid, and for minimum temperature in Barcelona. Minimum temperatures were found to have the greatest impact on UHI intensity. Using this temperature parameter, a mean UHI value of 2.3 °C was obtained in A Coruña, with similar values in Madrid and Granada (2.2 °C), although the former showed high extreme values of up to 11.7 °C. UHI intensity in Barcelona was slightly lower, and was around 1.9 °C. Conversely, intensity was much lower at the remaining

Table 5 UHI intensity for the most frequent synoptic patterns and the highest UHI values for each location in the study period

Station	Synoptic pattern/ The most frequent	UHI (°C)	Synoptic pattern/ The highest UHI	UHI (°C)
A Coruña	A	2.42	E	3.19
	U	2.23	AE	3.68
	E	3.19	SE	3.77
	C	2.01	ASE	3.82
Alicante	A	-0.21	CNW	0.33
	U	-0.30	CW	0.36
	E	-0.36	W	0.50
	C	-0.09	NW	0.51
Granada	A	1.47	ASW	1.36
	U	1.32	AE	1.39
	E	0.98	A	1.47
	C	0.50	ANE	1.51
Santander	A	1.72	S	2.26
	U	1.18	SE	2.59
	E	1.31	ASE	2.99
	C	0.91	AS	3.02
Valladolid	A	1.27	NW	1.94
	U	1.38	N	2.00
	E	1.28	ANW	2.04
	C	1.32	AN	2.27
Madrid	A	3.19	A	3.19
	U	2.69	SE	3.34
	E	2.29	AS	3.85
	C	1.01	ASE	4.28
Barcelona	A	2.20	SE	2.40
	U	1.78	ASE, W	2.42
	E	1.86	AW	2.52
	C	1.48	ASW	2.74

locations, with a value of 1.4 °C in Valladolid and 1.2 °C in Santander (the highest extreme value being 12.6 °C). The cooling effect of the UHI in Alicante was not noticeable and was -0.15 °C. The annual UHI trend was statistically significant (at a significance level of 0.001), with an increase of 0.023 °C/year in Valladolid and a smaller effect in Alicante, 0.009 °C/year. In contrast, a decreasing trend of -0.015 °C/year was observed in Santander. The study shows that UHI intensity results from the combined effect of urban density, topographical features, geographical location, and local air-flow conditions.

In general, statistically significant trends were found for all seasons in Valladolid, with the greatest increases occurring in spring and summer (around 0.03 °C/year). Alicante showed significant trends in most seasons except winter, although at a lower rate (up to 0.019 °C/year). Madrid showed a smaller trend in winter (0.012 °C/year). However, significant decreasing trends were observed in Barcelona for summer (-0.025 °C/year) and autumn (-0.028 °C/year), and in Santander for spring and summer (-0.024 and -0.025 °C/year, respectively).

Anticyclonic (A) and unclassified (U) weather situations were identified as the predominant synoptic patterns. The most pronounced effects of synoptic situations on the urban heat island –according to the Lamb classification– were mainly observed in hybrid patterns characterized by anticyclones and flows from the south, southeast, and southwest.

The highest mean UHI values were recorded in Madrid and A Coruña for the ASE type, with values of 4.3 and 3.8 °C, respectively. However, for the same synoptic pattern, the UHI in Santander was lower and reached 3.0 °C. The ASW synoptic pattern resulted in a mean UHI value of 2.7 °C. Moreover, in Valladolid, it was associated with the AN type (2.3 °C), and in Granada, with the ANE type (1.5 °C). Locations on the Mediterranean coast showed a different behaviour. In Barcelona, the UHI was influenced by hybrid anticyclonic conditions and westerly, and south-easterly flows. In contrast, in Alicante, although the UHI was generally not noticeable under most weather patterns, north-westerly flows and cyclonic situations did contribute to a certain extent. These findings indicate that both local geography and synoptic weather conditions play key roles in shaping UHI intensity.

Finally, this study seeks to provide evidence of the UHI phenomenon in southern Europe based on a dataset of seven Spanish cities with the aim of implementing policy strategies to mitigate the impact on people's lives and on the environment. Geographical location, city features, and local weather conditions prove key to understanding the potential effects of the urban heat island. With the support of different datasets and satellite imagery, it is therefore also important to continue exploring other scenarios and controlling factors so as to identify hot spots, particularly in large cities, in order to forecast extreme events and determine the most effective mitigation measures.

Supplementary Information The online version contains supplementary material available at <https://doi.org/10.1007/s00477-026-03205-2>.

Author contributions M. Ángeles García: Conceptualization, formal analysis, writing-original draft preparation. Isidro A. Pérez: Conceptualization, writing-reviewing & editing.

Funding Open access funding provided by FEDER European Funds and the Junta de Castilla y León under the Research and Innovation Strategy for Smart Specialization (RIS3) of Castilla y León 2021-2027. This research received no external funding.

Data availability Data are available from the ECAD&D web page: <https://www.ecad.eu/dailydata/predefinedseries.php>

Declarations

Conflict of interest The authors declare that they have no conflict of interest.

Open Access This article is licensed under a Creative Commons Attribution 4.0 International License, which permits use, sharing, adaptation, distribution and reproduction in any medium or format, as long as you give appropriate credit to the original author(s) and the source, provide a link to the Creative Commons licence, and indicate if changes were made. The images or other third party material in this article are included in the article's Creative Commons licence, unless indicated otherwise in a credit line to the material. If material is not included in the article's Creative Commons licence and your intended use is not permitted by statutory regulation or exceeds the permitted use, you will need to obtain permission directly from the copyright holder. To view a copy of this licence, visit <http://creativecommons.org/licenses/by/4.0/>.

References

- Agencia Estatal de Meteorología-España, Instituto de Meteorología-Portugal (2011) Atlas Climático Ibérico. Ministerio de Medio Ambiente, y Medio Rural y Marino, Madrid
- Almendros MA, López A (1995) La isla de calor en Madrid y las situaciones sinópticas. *Estud Geogr* 56:1–15. <https://doi.org/10.3989/egceogr.1995.i219.207>
- Andrade C, Fonseca A, Santos JA (2023) Climate change trends for the urban heat island intensities in two major Portuguese cities. *Sustainability* 15:3970. <https://doi.org/10.3390/su15053970>
- Aquino-Martínez LP, Ortega-Herrero B, Quintanar AI, Díaz-Esteban Y (2025) Synoptic patterns and heatwaves: intensity urban heat island in the Mexico Basin. *Urban Clim* 59:102318. <https://doi.org/10.1016/j.uclim.2025.102318>
- Arnds D, Böhner J, Bechtel B (2017) Spatio-temporal variance and meteorological drivers of the urban heat island in a European city. *Theor Appl Climatol* 128:43–61. <https://doi.org/10.1007/s00704-015-1687-4>
- Bushenkova A, Soares OMM, Johannsen F, Lima DCA (2024) Towards an improved representation of the urban heat island effect: a multi-scale application of XGBoost for Madrid. *Urban Clim* 55:101982. <https://doi.org/10.1016/j.uclim.2024.101982>
- Colangelo G, Sanesi G, Mariani L, Parisi SG, Cola G (2022) A circulation weather type analysis of urban effects on daily thermal range for Milan (Italy). *Atmosphere* 13:1529. <https://doi.org/10.3390/atmos13091529>
- Cuadrat JM, Martín VJ (2007) La Climatología Española: Presente y Futuro (Spanish climatology: past, present and future). *Prensas Universitarias de Zaragoza, Zaragoza*
- Cuadrat JM, Serrano-Notivol R, Barroo S, Saz MA, Tejedor E (2022) Variabilidad temporal de la isla de calor urbana de la ciudad de Zaragoza (España). *Cuadernos Investig Geogr* 48:97–110. <https://doi.org/10.18172/cig.5022>
- Cuerdo-Vilches T, Díaz J, López-Bueno JA, Luna MY, Navas MA, Mirón IJ, Linares C (2023) Impact of urban heat islands on morbidity and mortality in heat waves: observational time series analysis of Spain's five cities. *Sci Total Environ* 890:164412. <https://doi.org/10.1016/j.scitotenv.2023.164412>
- Fernández F, Almendros MA, López A (1996) La influencia del relieve en la isla de calor de Madrid: las vaguadas del Manzanares y del Abroñigal. *Estud Geogr* 57:473–494. <https://doi.org/10.3989/egceogr.1996.i224.682>
- García MA, Pérez IA, Hernández-Ceballos MA (2024) Heatwaves events and concurrent ozone concentrations between 2006 and 2022 at two sites in southern and northern Spain. *Environ Sci Pollut Res* 31:60819–60835. <https://doi.org/10.1007/S11356-024-35233-2>
- Hardin AW, Liu Y, Cao G, Vanos JK (2018) Urban heat island intensity and spatial variability by synoptic weather type in the northeast U.S. *Urban Climate* 24:747–762. <https://doi.org/10.1016/j.uclim.2017.09.001>
- Hidalgo D, Arco J (2022) Análisis espacio temporal de la Isla de Calor Urbana mediante imágenes satelitales: capitales de Andalucía. *ACE Archit City Environ* 17:1–30. <https://doi.org/10.5821/ace.17.49.10374>
- Jabbar HK, Hamoodi MN, Al-Hameedawi AN (2023) Urban heat islands: a review of contributing factors, effects and data. *IOP Conf Series: Earth Environ Sci* 1129(012038):1–9. <https://doi.org/10.1088/1755-1315/1129/1/012038>
- Jato-Espino D (2019) Spatiotemporal statistical analysis of the urban heat island in a Mediterranean region. *Sustain Cities Soc* 46:101427. <https://doi.org/10.1016/j.scs.2019.101427>
- Jones PD, Harpham C, Briffa KR (2013) Lamb weather types derived from reanalysis products. *Int J Climatol* 33:1129–1139. <https://doi.org/10.1002/joc.3498>
- Kundan MK, Sthool VA, Upadhye SK, Jadhav JD, Bagade SV, Giri AM (2020) Trend analysis of rainfall and rainy days using Mann Kendall Method and Sen's slope estimator in Parola Tehsil of Jalgaon District of Maharashtra (India). *Int J Curr Microbiol App Sci* 9:3038–3044. <https://doi.org/10.20546/ijemas.2020.912.36>
- Lamb HH (1972) British Isles weather types and a register of daily sequence of circulation patterns, 1861–1971. *Geophysical Memoir* 116, HMSO, London.
- Lehoczyk A, Sobrino JA, Skoković D, Aguilar E (2017) The urban heat island in the city of Valencia: a case study for hot summer days. *Urban Sci* 1:9. <https://doi.org/10.3390/urbansci1010009>
- Macintyre HL, Haviside C, Cai X, Phalkey R (2021) The winter urban heat island: impacts on cold-related mortality in a highly urbanized European region for present and future climate. *Environ Int* 154:106530. <https://doi.org/10.1016/j.envint.2021.106530>
- Maqueda G, Yagüe C, Román-Cascón C, Serrano E, Arrillaga JA (2020) Analysis of temperature trends and urban heat island in Madrid, EGU general assembly 2020, Online, 4–8 May 2020, EGU2020-10969. <https://doi.org/10.5194/egusphere-egu2020-10969>
- Marando F, Savatori E, Sebastiani A, Fusaro L, Manes F (2019) Regulation ecosystem service and green infrastructure: assessment of urban heat island effect mitigation in the municipality of Rome, Italy. *Ecol Model* 392:92–102. <https://doi.org/10.1016/j.ecolmodel.2018.11.011>
- Martinelli A, Kolokotsa DD, Fiorito F (2020) Urban heat island in Mediterranean coastal cities: the case of Bari (Italy). *Climate* 8:1–19. <https://doi.org/10.3390/cli8060079>
- Martínez J (2014) Estudio de la isla de calor de la ciudad de Alicante. *Investig Geogr (Alicante)* 62:83–99. <https://doi.org/10.14198/IN GEO2014.62.06>
- Martín-Vide J, Moreno MC, Artola VM, Cordobilla MJ (2016) Los tipos sinópticos de Jenkinson & Collinson y la intensidad de la isla urbana de calor barcelonesa. *X Congreso Internacional AEC: Clima, sociedad, riesgos y ordenación del territorio*. Jorge Olcina Cantos, Antonio M. Rico Amorós, Enrique Moltó Mantero (eds.). Universidad de Alicante. Instituto Interuniversitario de Geografía, Asociación Española de Climatología: 565–573. <https://doi.org/10.14198/XCongresoAECALicante2016-53>
- Martín-Vide J, Moreno-García MC (2020) Probability values for the intensity of Barcelona's urban heat island (Spain). *Atmos Res* 240:104877. <https://doi.org/10.1016/j.atmosres.2020.104877>
- Montávez JP, Rodríguez A, Jimenez JI (2000) A study of the urban heat island of Granada. *Int J Climatol* 20:899–911. [https://doi.org/10.1002/1097-0088\(20000630\)20:8%3c899::AID-JOC433%3e3.0.CO;2-I](https://doi.org/10.1002/1097-0088(20000630)20:8%3c899::AID-JOC433%3e3.0.CO;2-I)
- Moreno MC, Serra JA (2016) El estudio de la isla de calor en el ámbito mediterráneo: una revisión bibliográfica. *Biblio 3W. Rev Biblio Geogr Cienc Soc XXI* 1179:1–32

- Moreno-García MC (1994) Intensity and form of the urban heat island in Barcelona. *Int J Climatol* 14:705–710. <https://doi.org/10.1002/joc.3370140609>
- Núñez M, Sánchez-Guevara C, Neila FJ (2017) Update of the urban heat island of Madrid and its influence on the building's energy simulation. In: Mercader-Moyano P (ed) Sustainable development and renovation in architecture urbanism and engineering. Springer International Publishing, Berlin, pp 339–350
- Oke TR (1973) City size and the urban heat island. *Atmos Environ* 7:769–779. [https://doi.org/10.1016/0004-6981\(73\)90140-6](https://doi.org/10.1016/0004-6981(73)90140-6)
- Pérez IA, García MA (2023) Climate change in the Iberian Peninsula by weather types and temperature. *Atmos Res* 284:1–10. <https://doi.org/10.1016/j.atmosres.2022.106596>
- Pérez IA, García MA, Rasekhi S, Pazoki F, Fernández-Duque B (2024) Extension and trend of the London urban heat island under Lamb weather types. *Sustain Cities Soc* 114:1–14. <https://doi.org/10.1016/j.scs.2024.105743>
- Roca J, Arellano B, Zhang X (2023) Global warming in Spanish cities (1971–2022), EGU General Assembly 2023, Vienna, Austria, 23–28 Apr 2023, EGU23-16349. <https://doi.org/10.5194/egusphere-egu23-16349>, 2023.
- Román E, Gómez G, de Luxán M (2017) Urban heat island of Madrid and its influence over urban thermal comfort. In: Mercader-Moyano P (ed) Sustainable development and renovation in architecture, urbanism and engineering. Springer International Publishing, Berlin, pp 415–425
- Runnalls KE, Oke TR (2000) Dynamics and controls of the near-surface heat island of Vancouver, British Columbia. *Phys Geogr* 21:283–304
- Salmi T, Maatta A, Anttila P, Airola R, Amnell T (2002) Detection trends of annual values of atmospheric pollutants by the Mann Kendall test and Sen's slope estimates the Excel template application MAKESENS. Finnish Meteorological Institute Air Quality Research, 1–35.
- Salvati A, Roura HC, Cecere C (2017) Assessing the urban heat island and its energy impact on residential buildings in Mediterranean climate: Barcelona case study. *Energy Build* 146:38–54. <https://doi.org/10.1016/j.enbuild.2017.04.025>
- Santamouris M (2015) Analyzing the heat island magnitude and characteristics in one hundred Asian and Australian cities and regions. *Sci Total Environ* 512–513:582–598. <https://doi.org/10.1016/j.scitotenv.2015.01.060>
- Santamouris M (2020) Recent progress in urban heating research. Integrated assessment of the energy, environmental, vulnerability and health impact. Synergies with the global climate change. *Energy Build* 207:109482. <https://doi.org/10.1016/j.enbuild.2019.109482>
- Santamouris M, Kolokotsa D (2015) On the impact of urban overheating and extreme climatic conditions on housing, energy, comfort and environmental quality of vulnerable population in Europe. *Energy Build* 98:125–133. <https://doi.org/10.1016/j.enbuild.2014.08.050>
- Santamouris M, Papanikolaou N, Livada I, Koronakis I, Georagnis C, Argiriou A, Asimakopoulos DN (2001) On the impact of urban climate on the energy consumption of buildings. *Sol Energy* 70:201–216. [https://doi.org/10.1016/S0038-092X\(00\)00095-5](https://doi.org/10.1016/S0038-092X(00)00095-5)
- Sen PK (1968) Estimation of regression coefficient based on Kendall's Tau. *J Am Stat Assoc* 63:1379–1389. <https://doi.org/10.2307/2285891>
- Sobrino JA, Sòria G, Oltra-carrió R, Jiménez-Muñoz JC, Cuenca J et al (2009) DESIREX 2008: Estudio de la isla de calor en la Ciudad de Madrid. *Rev Teledetec* 31:80–92
- Su SH, Chu JL, Yo TS, Lin LY (2018) Identification of synoptic weather types over Taiwan area with multiple classifiers. *Atmos Sci Lett* 19:e861: 1–6. <https://doi.org/10.1002/asl.861>
- Tehrani AA, Veisi O, Kia K, Delavar Y, Bahrami S, Sobhaninia S, Mehan A (2024) Predicting urban heat island in European cities: a comparative study of GRU, DNN, and ANN models using urban morphological variables. *Urban Climate* 56:102061. <https://doi.org/10.1016/j.uclim.2024.102061>
- Tzavali A, Paravantis JP, Mihalakakou G, Fotiadi A, Stigka E (2015) Urban heat island intensity: a literature review. *Fresenius Environ Bull* 24:4537–4554
- Wang WC, Zeng Z, Karl TR (1990) Urban heat islands in China. *Geophys Res Lett* 17:2377–2380. <https://doi.org/10.1029/GL017i013p02377>
- Ward K, Lauf S, Kleinschmit B, Endlicher W (2016) Heat waves and urban heat islands in Europe: a review of relevant drivers. *Sci Total Environ* 569–570:527–539. <https://doi.org/10.1016/j.scitotenv.2016.06.119>
- WHO (2021) Heat and health in the WHO European Region: updated evidence for effective prevention. In: Martínez, G. Sanchez, De'Donato, F., Kendrovski, V. (Eds.), WHO Regional Office for Europe Copenhagen: WHO Regional Office for Europe. Licence: CC BY-NC-SA3.0 IGO. <https://apps.who.int/iris/bitstream/handle/10665/339462/9789289055406-eng.pdf>
- Wilby RL (2003) Past and projected trends in London's urban heat island. *Weather* 58:251–260. <https://doi.org/10.1256/wea.183.02>
- Yagüe C, Zurita E, Martínez Z (1991) Statistical analysis of the Madrid urban heat island. *Atmos Environ* 25B(3):327–332. [https://doi.org/10.1016/0957-1272\(91\)90004-X](https://doi.org/10.1016/0957-1272(91)90004-X)
- Yang Y, Guo M, Ren G, Liu S, Zong L, Zhang Y, Zheng Z, Miao Y, Zhang Y (2022) Modulation of wintertime canopy urban heat island (CUHI) intensity in Beijing by synoptic weather pattern in planetary boundary layer. *J Geophys Res Atmos* 127:e2021JD035988. <https://doi.org/10.1029/2021JD035988>
- Yue W, Liu X, Zhou Y, Liu Y (2019) Impacts of urban configuration on urban heat island: an empirical study in China mega-cities. *Sci Total Environ* 671:1036–1046. <https://doi.org/10.1016/j.scitotenv.2019.03.421>

Publisher's Note Springer Nature remains neutral with regard to jurisdictional claims in published maps and institutional affiliations.